Int. J. Electrochem. Sci., 11 **(2016)** 1213 - 1227

International Journal of
ELECTROCHEMICAL
SCIENCE
www.electrochemsci.org

Influence of Oxidation Stage and Exfoliation Extent of Carbon-Based Materials on Electrochemical Detection of As(III)

Monika Kremplova[1,2], *Lukas Richtera*[1,2], *Pavel Kopel*[1,2], *Renata Kensova*[1,2], *Iva Blazkova*[1,2], *Vedran Milosavljevic*[1], *David Hynek*[1,2], *Vojtech Adam*[1,2], *Rene Kizek*[1, 2*]

[1] Department of Chemistry and Biochemistry, Faculty of Agronomy, Mendel University in Brno, Zemedelska 1, CZ-613 00 Brno, Czech Republic, European Union
[2] Central European Institute of Technology, Brno University of Technology, Technicka 3058/10, CZ-616 00 Brno, Czech Republic, European Union
[*]E-mail: kizek@sci.muni.cz

Received: 5 May 2015 / *Accepted:* 23 May 2015 / *Published:* 1 January 2016

This study deals with the electrochemical detection of As(III) and especially with its interaction with carbon-based materials such as graphene oxide, graphite oxide and partially reduced graphene oxide in connection with the adsorption of As(III) to their surface. Using differential pulse voltammetry and atomic absorption spectrometry, it was found that the As(III) reaches the best adsorption efficiency on the carbon-based materials surfaces at very acidic pH after 1 hour interaction. We decided to use this promising ability of graphene oxide to design a new method for As(III) detection using a modified glassy carbon electrode (GCE). In order to enable detection of As(III), the surface of glassy carbon electrode was firstly modified by gold nanoparticles (AuNPs). After this step the working electrode was modified for with graphene oxide to enhance the electrochemical signal of As(III). Compared to the working electrode modified only by gold nanoparticles, the electrochemical signal of As(III) on the GCE/AuNPs/GO increased by approx. 50%. Interaction time of As(III) on graphene oxide (located on the surface of the working electrode) demonstrated the process of As(III) adsorption to the surface, which is manifested by increasing electrochemical signal of As(III) in individual time intervals.

Keywords: arsenic, graphene oxide, reduced graphene oxide, gold nanoparticles, glassy carbon electrode, differential pulse voltammetry

1. INTRODUCTION

Arsenic in the form of non-volatile inorganic compounds occurs naturally in the Earth's crust [1]. At low concentrations, it may be present in the aquatic environment and in atmosphere mostly due to weathering and erosion of rocks and minerals, volcanic activity and biological processes [2,3].

Higher concentrations of arsenic in the environment result from anthropogenic activities. Its occurrence is mainly associated with the combustion of fossil fuels and metallurgical processes [1-3]. Appreciable concentrations of arsenic are released during burning of wood treated by chemicals containing arsenic compounds, or with pesticide application [4,5]. In surface water and groundwater arsenic exists in both organic and inorganic forms in the oxidation states of As(III) - arsenite and As(V) – arsenate [6]. The most common organic forms include monomethylarsonic acid and dimethylarsinic acid [1,7] which arise biosynthetically, mostly as a metabolic product of microorganisms [8-10]. Inorganic forms of arsenic occur in natural waters more often and exhibit higher toxicity than organic forms.

In many countries of the world, higher levels of arsenic exceeding the permitted limits were recorded in industrial and drinking water, vegetables, cereals, fish, meat and milk [11-15]. Arsenic toxicity is the cause of a number of diseases and tissue damage, such as atherosclerosis, hypertension, skin lesions, mucous membrane disorders and nervous system damage [16-19]. Excessive exposure to arsenic can lead to gastrointestinal and cardiovascular problems, and in the worst cases can have genotoxic, mutagenic and carcinogenic effects [20-22].

With regards to environmental importance of arsenic, new ways of detection offering fast, inexpensive and routine detection of this element are of high importance, as well as the optimization of existing processes for detection of arsenic to increase the sensitivity and reproducibility. Nowadays there is a number of methods usable for detection of arsenic, e.g. atomic fluorescence spectrometry [23-25], hydride generation-atomic absorption spectrometry (HG-AAS) [26,27], inductively coupled plasma mass spectrometry [28-31], electrospray mass spectrometry [32]. These methods are high-cost, require expensive laboratory equipment, frequently a complicated sample preparation is required, and last but not least, they tend to be time consuming. A preferred alternative to these techniques may be electrochemical methods with the advantage of easy handling, high sensitivity of determination and the relatively low cost with the low price of individual determination. It is possible to determine both As(III) and As(V) forms of arsenic electrochemically, however it requires chemical pretreatment of As(V) in the sample to As(III) form [33]. For the determination of arsenic in aqueous solutions several electrochemical methods like cyclic voltammetry (CV), differential pulse voltammetry, linear sweep voltammetry, square wave voltammetry and various types of working electrodes (mercury, glassy carbon, gold, etc.) can be used [34-37]. The advantage of solid-state electrodes is a possibility of modifications using different kinds of nanomaterial [38-40], which allows increasing the sensitivity of detection.

The aim of this study is the monitoring of the trivalent arsenic, especially its adsorption on the surface of the carbon-based materials such as graphene oxide, graphite oxide and partially reduced graphene oxide. The method used for As(III) determination after the interaction with carbon based materials was differential pulse voltammetry on hanging mercury drop electrode. Selected carbon-based material with best adsorption properties was further used for second modification of glassy carbon electrode. For determination of As(III) on glassy carbon electrode, this electrode was firstly modified by gold nanoparticles and next the second modification step was based just on the carbon material to increase the sensitivity of the electrochemical determination of As(III) using the ability of its adsorption onto the sorbent surface.

2. EXPERIMENTAL PART

2.1 Chemicals and material

All chemicals used in this study were purchased from Sigma Aldrich (St. Louis, MA, USA) in ACS purity unless noted otherwise. Pipetting was performed by pipettes from Eppendorf (Hamburg, Germany). Stock solutions were prepared with ACS water. High purity deionized water (Milli-Q Millipore 18.2 MΩ/cm, Bedford, MA, USA) was used for rinsing, washing, and buffer preparation, pH values were measured using an inoLab Level 3 (Wissenschaftlich-Technische Werkstatten GmbH, Weilheim, Germany).

2.2. Preparation of graphite oxide

The preparation of graphite oxide was done according to the standard method of Hummers [41]. The graphite (2 g) was added to 46 mL of concentrated sulfuric acid and mixed by stirring and cooled with ice, followed by an addition of 1 g $NaNO_3$ and 6 g of $KMnO_4$. The mixture was left for 24 h at laboratory temperature, in order to thicken it. All the black graphene oxide was stirred in 300 mL of ACS water.

2.3. Preparation of graphene oxide

Graphite oxide for graphene oxide (GO) synthesis was prepared by chemical oxidation of 5.0 g graphite flakes in a mixture of concentrated H_2SO_4 (670 mL) and 30 g $KMnO_4$ according to the simplified Hummer's method [42]. The reaction mixture was stirred vigorously. The oxidation process manifests outwardly by the gradual color change from dark purplish green to dark brown. After 4 days, the oxidation of graphite was terminated by slow addition of H_2O_2 solution (250 mL) and the color of the mixture turned to bright yellow, indicating high oxidation level of graphite. Formed graphite oxide was washed 3 times with 1 M of HCl and repeatedly several times washed with deionized water (total volume used - 12 L) until constant pH value (3–4) was achieved using a simple decantation until it was possible and using centrifugation at the last steps. During the washing process with deionized water exfoliation of graphite oxide led to the thickening of solution and formation of stable colloid of graphene oxide.

2.4. Preparation of partially reduced graphene oxide

The synthesis of partially reduced GO was performed according to the Gao at al. [43] procedure but simplified. Solution of graphene oxide was diluted with deionized water to concentration 1 g/L (total volume 140 cm^3) and pH of solution was adjusted by 5% sodium carbonate solution to value 9.5. Sodium borohydride (1.15 g, reagent grade, 98.5%, Sigma-Aldrich) was slowly added into the solution under magnetic stirring and then heated to 80°C. Reaction mixture was kept at this temperature and under stirring for 3 h (till the formation of gaseous products can be observed).

The reduction process was manifested by turning brown color of solution to black. Reduced product was washed with deionized water to remove impurities and separated by centrifugation several times until constant pH value (6–7) was achieved.

2.5. Preparation of samples for interaction with As(III) in different pH values

250 μL (5 mg/mL) of carbon material (graphite oxide, graphene oxide, partially reduced graphene oxide) was mixed with 375 μL of As(III) standard solution (100 μM) and followed by addition of 375 μL ACS water, hydrochloric acid or sodium hydroxide depending on required pH value. Interaction of As(III) compound and carbon materials was carried out for 1 hour under shaking (BIOSAN, Multi RS-60) at room temperature. After the interaction, the sample was centrifuged (BIOSAN, FVL 2400N, Combi-Spin) for 30 min. The supernatant was carefully removed using a syringe with a needle and filtered through a membrane filter (0.45 μm). The concentration of As(III) in supernatant was detected by differential pulse voltammetry and compared with applied As(III) concentration to observe the rate of adsorption.

2.6. Preparation of samples for time-interaction with As(III)

250 μL (5 mg/mL) of carbon materials (graphite oxide, graphene oxide, partially reduced graphene oxide) was mixed with 375 μL of As(III) standard solution (100 μM) followed by addition of 375 μL of concentrated hydrochloric acid. Interaction of arsenic and carbon material was carried out in five different time intervals (0, 30, 60, 90 and 120 minutes). Shaking, centrifugation, filtration and As(III) determination was carried out under the same conditions as reported in section *2.5.* (see above).

2.7. Preparation of gold nanoparticles

19.7 mg $HAuCl_4 \cdot 3H_2O$ was dissolved in 50 mL of Milli-Q water to form yellow solution (1 mM) followed by addition 1.25 mL of sodium citrate solution (0.1 M) was added. Reaction mixture was stirred for 1 h at ambient temperature until the color of the solution turned purple [44].

2.8. Preparation of modified glassy carbon electrode

For modification of glassy carbon electrode, gold nanoparticles and graphene oxide were used. At the first step, the surface of GCE was thoroughly polished using Alumina powder 0.05 μm (CH Instruments, USA). On the clean GCE surface drop of AuNPs solution was applied and the fluid was slowly evaporated at 30°C to form thin AuNPs layer. The second step of the modification included covering the AuNPs layer with graphene oxide. Therefore, drop of graphene oxide suspension was applied onto dried AuNPs layer and after subsequent evaporation of fluid at 30°C the modified GCE was ready to use.

2.9. Electrochemical determination of Arsenic using hanging mercury drop electrode

Determination of As(III) by differential pulse voltammetry were performed with 797 VA Computrace (Metrohm, Switzerland), using a standard cell with three electrodes. A hanging mercury drop electrode with a drop area of 0.4 mm^2 was the working electrode. An Ag/AgCl/3M KCl electrode was the reference and platinum electrode was auxiliary. For data processing 797 VA Computrace software by Metrohm CH was employed. The analyzed samples were deoxygenated prior to measurements by purging with argon (99.999%). 0.75 M hydrochloric acid with addition of $CuSO_4$ (1g/L) as a supporting electrolyte was used. The supporting electrolyte was exchanged after each analysis. The parameters of the measurements were as follows: initial potential of -0.1 V, end potential - 1.2 V, deoxygenating with argon 120 s, deposition 0 s, pulse amplitude 0.05 V, pulse time 0.04 s, voltage step 0.003 V, voltage step time 0.4 s, sweep rate 0.0076 V/s, volume of injected sample: 20 µL, volume of injected $CuSO_4$: 110 µL, volume of measuring cell 2 mL (20 µL of sample + 110 µL of $CuSO_4$ + 1870 µL acetate buffer).

2.10. The microscopy of complexes in ambient light

The inverted system microscope Olympus UIS2 series (Tokyo, Japan) was used for the imaging of the carbon materials. Samples were pipetted on a microscope slide and covered by a cover slip. The objective CPlanFLN 10× (N.A. 0.3, W.D. 9.5 mm, F.N. 22) was used for magnification 100× and objective LUCPlanFLN 40× (N.A. 0.6, W.D. 2.7 – 4 mm, F.N. 22) was used for magnification 400×. The images were captured by Camera Olympus DP73 and processed by Stream Basic 1.7 Software, the resolution of the images was 1600 × 1200 pixels, ISO 200.

2.11. Scanning electron microscopy (SEM)

Structure of carbon materials was characterized by SEM. For documentation of the structure, a MIRA3 LMU (Tescan, Brno, Czech Republic) was used. The SEM was fitted with In-Beam SE detector. An accelerating voltage of 15 kV and beam currents about 1 nA gave satisfactory results.

2.10. Electrochemical determination of As(III) using modified glassy carbon electrode

Determination of As(III) by linear sweep voltammetry was performed by CH Instruments Electrochemical Workstation (CH Instruments, USA) using a system of 3 electrodes. A modified glassy carbon electrode was used as the working electrode; an Ag/AgCl/3M KCl was used as the reference electrode, and a platinum wire as an auxiliary one. The analyzed samples were deoxygenated prior to measurements using 99.999% argon for 120 s and 0.75 M hydrochloric acid was used as supporting electrolyte. The parameters of the measurement were chosen as follows: initial potential of -0.4 V, end potential 0.5 V, sample interval 0.001 V, preconditioning potential -0.4 V, deposition time

60 s, scan rate 0.1 V/s. Volume of injected sample: 20 μL, volume of electrochemical cell was 2 mL (20 μL of sample + 1980 μL of electrolyte).

2.11. Atomic absorption spectrometry (AAS)

Total arsenic was determined on 280Z Agilent Technologies atomic absorption spectrometer (Agilent, USA) with electrothermal atomization. Arsenic ultrasensitive hollow cathode lamp (Agilent) was used as the radiation source (lamp current 10 mA). The spectrometer was operated at 193.7 nm resonance line with spectral bandwidth of 0.5 nm. The sample volume of 20 μL was injected into the graphite tube. The flow of argon inert gas was 300 mL/min. Zeeman background correction was used with field strength of 0.8 Tesla. Arsenic was determined in the presence of palladium chemical modifier.

3. RESULTS AND DISCUSSION

Materials based on graphene oxide and reduced graphene oxide exhibit convenient sorption abilities towards heavy metals, which can be used e.g. for decontamination of surface water and wastewater polluted by these metals. Promising sorption capacity has been also reported to other substances and elements of metallic or non-metallic nature [45-47]. Mentioned adsorption ability is also one of the key steps in the determination of electrochemically active compounds. In electrochemical assays, several physico-chemical processes, e.g. diffusion, oxidation-reduction processes, the preconcentration of an analyte on electrode surface by preliminary electrolysis, and finally adsorption are used [48,49]. Carbon-based materials (graphite oxide, graphene oxide, partially reduced graphene oxide) were used for interacting with arsenic and for subsequent study of the electrochemical behavior of this transition metal in their presence, due to their sorption abilities and surface characteristics. It was expected, if the material exhibits a sorption ability towards specific substance, it could be also a promising material for modification of the working electrode designed for the detection of given analyte. With respect to these facts, three carbon-based materials were studied and the material with the best qualities was then selected for modification of the glassy carbon electrode.

3.1. Electrochemical determination of As(III) using hanging mercury drop electrode

For detection of arsenic in aqueous solutions and for the verification of sorption properties of carbon-based materials, an electrochemical method differential pulse voltammetry as one of the most sensitive techniques for the determination of metal ions, metalloids and other electrochemically active substances have been used [50,51]. As a standard, solution of trivalent arsenic $AsCl_3$ was used. The addition of chloride hydrazine as the reducing agent is necessary in order to avoid spontaneous oxidation of trivalent arsenic to a higher oxidation state. For the electrochemical determination of

As(III) on the mercury working electrode there is strictly necessary to add Cu(II) ions, which leads to the formation of the copper amalgam on the surface of the mercury electrode, and subsequently to form an intermetallic compounds Cu_3As_2. At highly acidic pH used in cathodic stripping voltammetry, this compound passes into AsH_3, which provides an electrochemical signal [36].

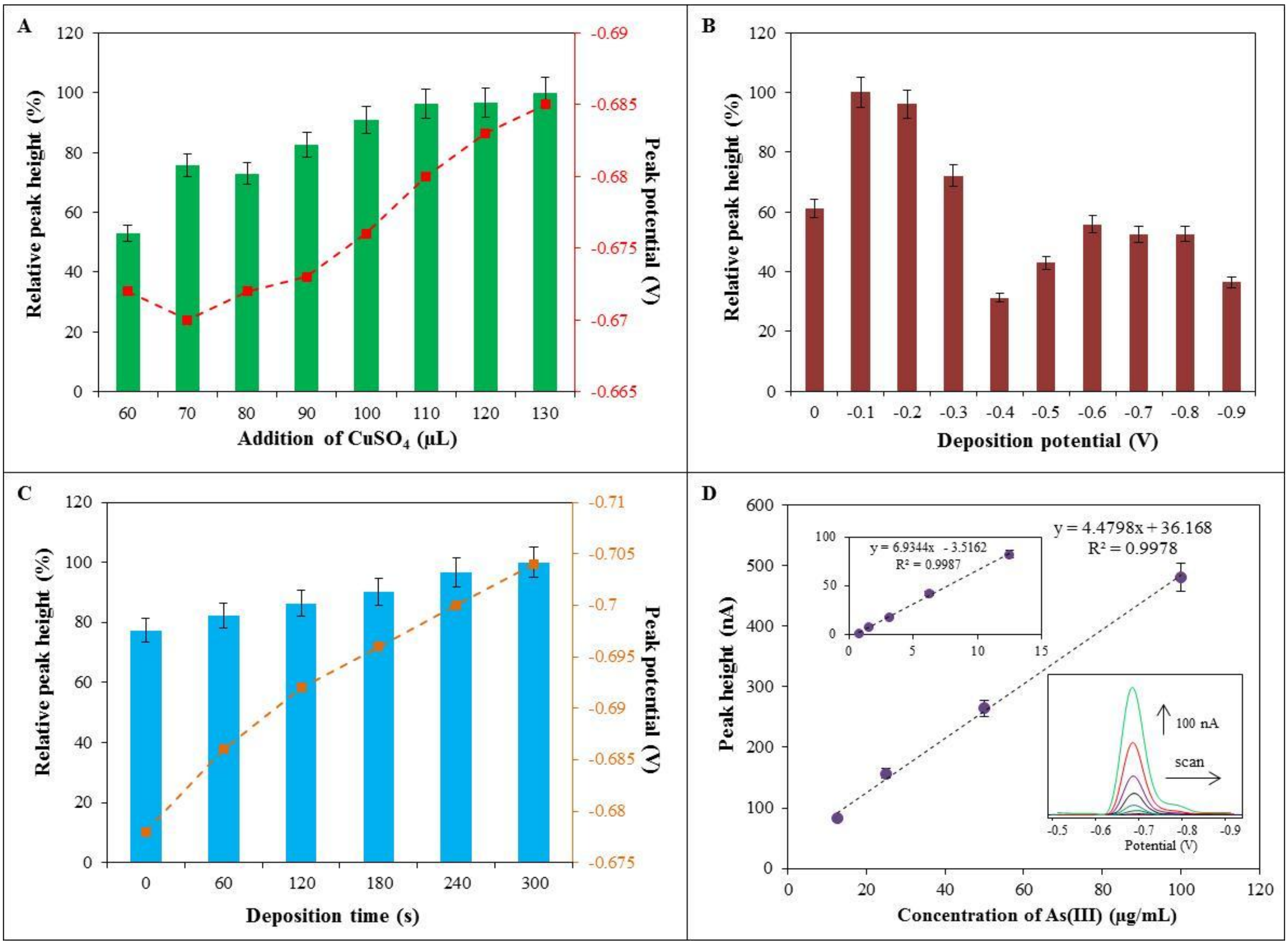

Figure 1. Optimization of the parameters of the method for As(III) determination: **(A)** dependence of relative peak height on the addition of $CuSO_4$ (1g/L), red points indicates a potential values of As(III) peak; **(B)** influence of deposition potential (0, -0.1, -0.2, -0.3, -0.4, -0.5, -0.6, -0.7, -0.8 and -0.9 V) on relative peak height of As(III); **(C)** dependence of relative peak height of As(III) on deposition time (0, 60, 120, 180, 240 and 300 s); **(D)** calibration curves in concentration range 0.78 – 12.5 µg/mL and 12.5 – 100 µg/mL containing inserted voltammograms (each line for one measured concentration in concentration range 0.78 – 100 µg/mL, measured by differential pulse voltammetry). 0.75 M hydrochloric acid with $CuSO_4$ addition (1g/L) was used as a supporting electrolyte. Parameters of the method were as follows: initial potential -0.1 V, end potential - 1.2 V, deoxygenating with argon 120 s, deposition 0 s, pulse amplitude 0.05 V, pulse time 0.04 s, voltage step 0.003 V, voltage step time 0.4 s, sweep rate 0.0076 V/s.

For obtaining a higher sensitivity of the method, an individual parameters were optimized. The addition of copper ions was the first optimized parameter because Cu(II) ions influence the intensity and the quality of the obtained electrochemical signal of As(III). The volume of added $CuSO_4$

(concentration of Cu(II) 1g/L) to the supporting electrolyte was gradually increased in the range 60 - 130 mL. From Figure 1A, it is clear that with increasing concentration of Cu(II) ions in the electrolyte the electrochemical signal of As(III) increased and the peak potential shifted to more negative values. The highest signal was obtained by the volume of 130 mL, but at this point an unstable potential of the characteristic peak of As(III) was recorded. At applied volume of 110 mL, stable electrochemical response was recorded and for this reason, this volume of $CuSO_4$ was used for all other electrochemical determination of As(III) using a mercury electrode.

Further, the deposition potential was tested (Figure 1B) in the values 0; -0.1; -0.2; -0.3; -0.4; -0.5; -0.6; -0.7; -0.8 and -0.9 V. In this case, there was no dependence between the electrochemical signal of As(III) and decreasing values of the applied potential. The best electrochemical response was observed at deposition potential -0.1 V that was also selected as an initial potential during this method. Deposition time associated with deposition potential was the next optimized parameter. Figure 1C shows an increasing electrochemical signal of As(III) depending on the increasing deposition time. The peak potential was shifted to more negative values. The increase in the peak height of As(III) (compared zero) and the maximum applied deposition time did not exceed 25%, therefore considering the length of the individual assay the deposition time of 0 s was used in all subsequent measurements.

After optimization steps, the calibration curve of As(III) in concentration range 0.78 – 100 µg/mL was determined. Due to the relatively wide concentration range, two areas of the calibration curve with a linear course were selected. Between 12.5 – 100 µg/mL the concentration dependence has a linear course with regression equation $y = 4.4798x + 36.168$ ($n = 4$) and coefficient of determination $R^2 = 0.9978$. A calibration curve in the lower concentration range (0.78 – 12.5 µg/mL) with linear course, regression equation $y = 6.9344x – 3.5162$ and coefficient of determination $R^2 = 0.9987$ is shown in the upper inset of the Figure 1D. . Characteristic peak of As(III) was detected in potential of -0.68 V. Characteristic voltammograms are shown in the lower inset of Figure 1D.

3.2. Characterization of carbon-based materials using microscopy in ambient light and SEM analysis

In this study, the carbon-based materials such as graphite oxide, graphene oxide and partially reduced graphene oxide were used because of their sorption properties and high surface area. For verification of the carbon materials structure, the microscopy in an ambient light and SEM analysis were used. Using microscopy in the ambient light, the Figure 2Aa (magnification 100×) shows particles with size of several micrometers. Darker particles represent unexfoliated material (graphite oxide) which does not meet the parameters of nanoparticles. At higher magnification (Figure 2Ab, magnification 400×) disparate thickness of individual particles is more evident, while larger lightproof particles probably contain a higher proportion of non-oxidized graphite. In the case of graphene oxide in Figure 2Ba particle sizes were much smaller than in the previous case, the fundamental difference is greater homogeneity of the sample and only a minor presence of particles with high thickness. The graphene oxide nanoparticles are very thin due to almost perfect exfoliation, their thickness not exceeding units or tens of nanometers, and therefore their edges are typically less recognizable for microscopy in ambient light (Figure 2Bb).

Figure 2Ca represents the structure of the partially reduced graphene oxide. For synthesis of this carbon-based material graphene oxide (Figure 2Ba, 2Bb) as starting compound was used. During reduction process the agglomeration of GO individual nanoparticles occur due to the loss of polar functional groups on GO surface, leading to reduced solubility in aqueous medium. Nevertheless, in comparison with Figures 2Aa and 2Ab, partially reduced graphene oxide has a much finer structure. These observations are fully consistent with the results of SEM analysis.

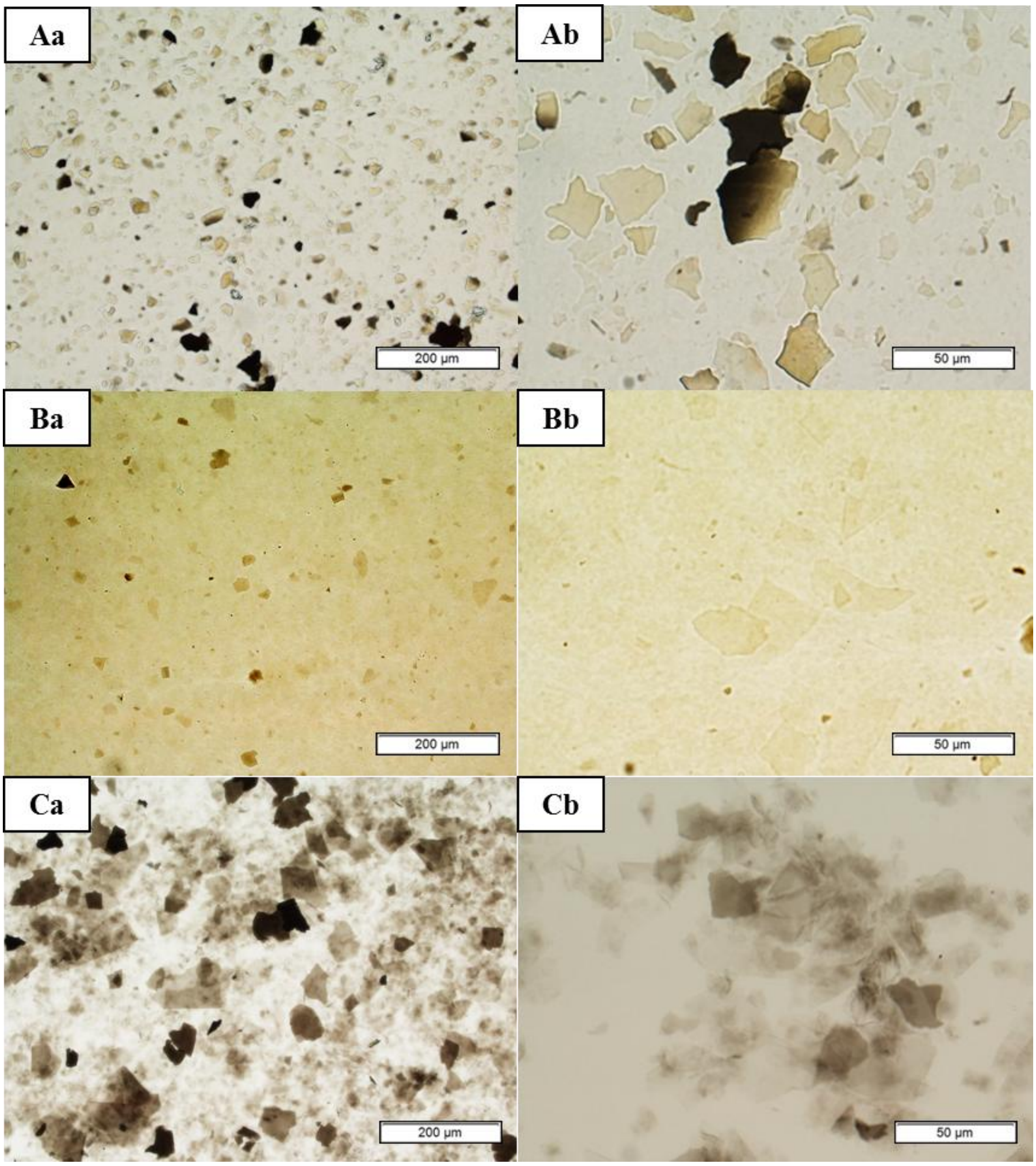

Figure 2. Micrographs of carbon materials using microscopy in ambient light: **(A)** graphite oxide; **(B)** graphene oxide; **(C)** partially reduced graphene oxide. Parameters were as follows: Device: Microscopy; Zoom: 100× (“a” labelled micrographs) or 400× (“b” labelled micrographs); Ambient light; ISO 200; Resolution: 1600 × 1200.

For a more detailed description of the structure of carbon materials, SEM analysis was used. Figure 3 shows representative SEM micrographs that express the morphology of individual carbon materials obtained by drying dispersions on clean silicon wafers.

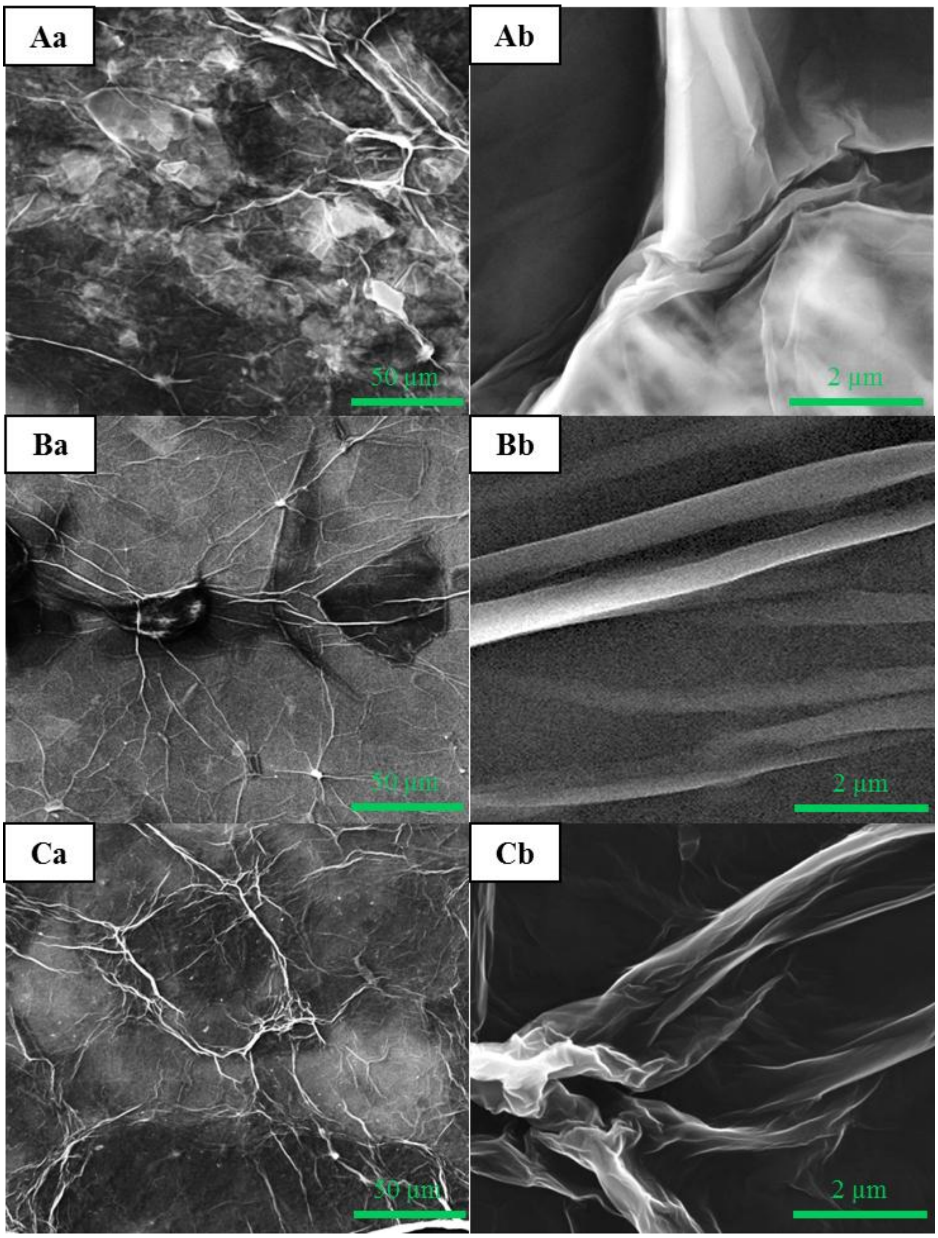

Figure 3. SEM micrographs of **(A)** graphite oxide, **(B)** graphene oxide, **(C)** partially reduced GO with their representative morphology obtained by drying of appropriate dispersions on clean silicon wafers. Magnification (a) 1000×, (b) 30 000×, standard detection mode SEI (secondary electron imaging).

Using 1000× magnification in Figure 3Aa was noticeable bumpy surface of a material caused by the uneven distribution of the size and thickness of the individual particles of graphite oxide. Nevertheless it can be seen that this material contains partially exfoliated proportion, which shows only locally transparent veil structure at 30 000× (Figure 3Ab). Figure 3Ba (1000× magnification) shows the characteristic structure formed by evaporating the solvent from a solution of graphene oxide. Formed continuous layer tends to be transparent in the case of the residue from the solution with a low concentration of solids and the substrate (silicon wafers) can be observed under this layer. Detailed photo (Figure 3Bb) also shows the transparent veil undulating morphology characteristic for graphene oxide [52]. The structure of the partially reduced graphene oxide (Figure 3C) is quite similar to the starting material (Figure 3B), but it is clearly visible that the partially reduced graphene oxide have more pronounced gossamer texture (Figure 3Ca) even at magnification 30 000× (Figure 3Cb). These structural changes are consistent with the chemical changes that occur during the process of reduction of graphene oxide.

3.3. Interaction of carbon-based materials with As(III) depending on pH

To improve the efficiency of the detection method, in general it is required to modify the carbon material, which forms the working electrode. Characterization of the behavior of these materials in the presence of analyzed samples is a crucial step. For this reason, the interaction of carbon-based materials with As(III) in the pH range 0-7 was carried out. The acidic medium was chosen according to the electrochemical determination of As(III). The ability of carbon-based materials to adsorb As(III) ions on a carbon surface was investigated (Figure 4).

A standard solution of As(III) was added to individual aliquots of graphene oxide, graphite oxide and the partially reduced graphene oxide, the mixtures were shaken for one hour. After this time the concentrations of As(III) was determined by difference pulse voltammetry and atomic absorption spectrometry in the filtered supernatant. The graph in Figure 4A shows the strongest adsorption onto the carbon surface at the lowest pH (the value was approximated to zero for all three carbon materials). The available literature shows that the adsorption of As(III) to the sorption materials is strongly influenced by the pH of the environment caused by dissociation H_3AsO_3 gradually to $H_2AsO_3^-$, $HAsO_3^{2-}$ and finally in a strongly basic region to AsO_3^{3-}. Generally, at alkaline pH the adsorption of As(III) occurs with a higher efficiency than at the acidic range, but the character of the sorbent and dissociation groups respectively the charge on its surface also plays the important role [53]. However, due to the electrochemical determination of As(III) using the glassy carbon electrode, which takes place at very low pH, the adsorption studies of the behavior of As(III) to the surface of the carbon material was carried out in strongly acidic to neutral environment.

For the graphene oxide, the adsorption efficiency was determined as 24.6%, for graphite oxide - 18.1% and for partially reduced graphene oxide - 13.4% after the interaction time of one hour. Adsorption efficiency of As(III) to the surface of carbon-based materials was not higher in comparison with the values obtained at the most acidic pH.

For maximum efficiency of adsorption, substantially acidic pH created by the addition of concentrated HCl to the sample, was used in following experiment. The interaction between carbon-based materials and As(III) in different reaction times was investigated in order to ascertain optimal interaction time when the surface adsorption is utmost. For this experiment, 5 different interaction times (0; 30; 60; 90 and 120 minutes) were used. From Figure 4Bb can be seen that in the time range of 60-90 minutes, the efficiency of adsorption reached the maximum which is comparable to others carbon based materials [54]. Graphene oxide with the adsorption efficiency of 30.8% after 1 hour interaction seemed to be the most effective and this trend was confirmed by atomic absorption spectrometry (Figure 4Ba). This material was used for modification of glassy carbon electrode used in the electrochemical detection of As(III) in aqueous solutions.

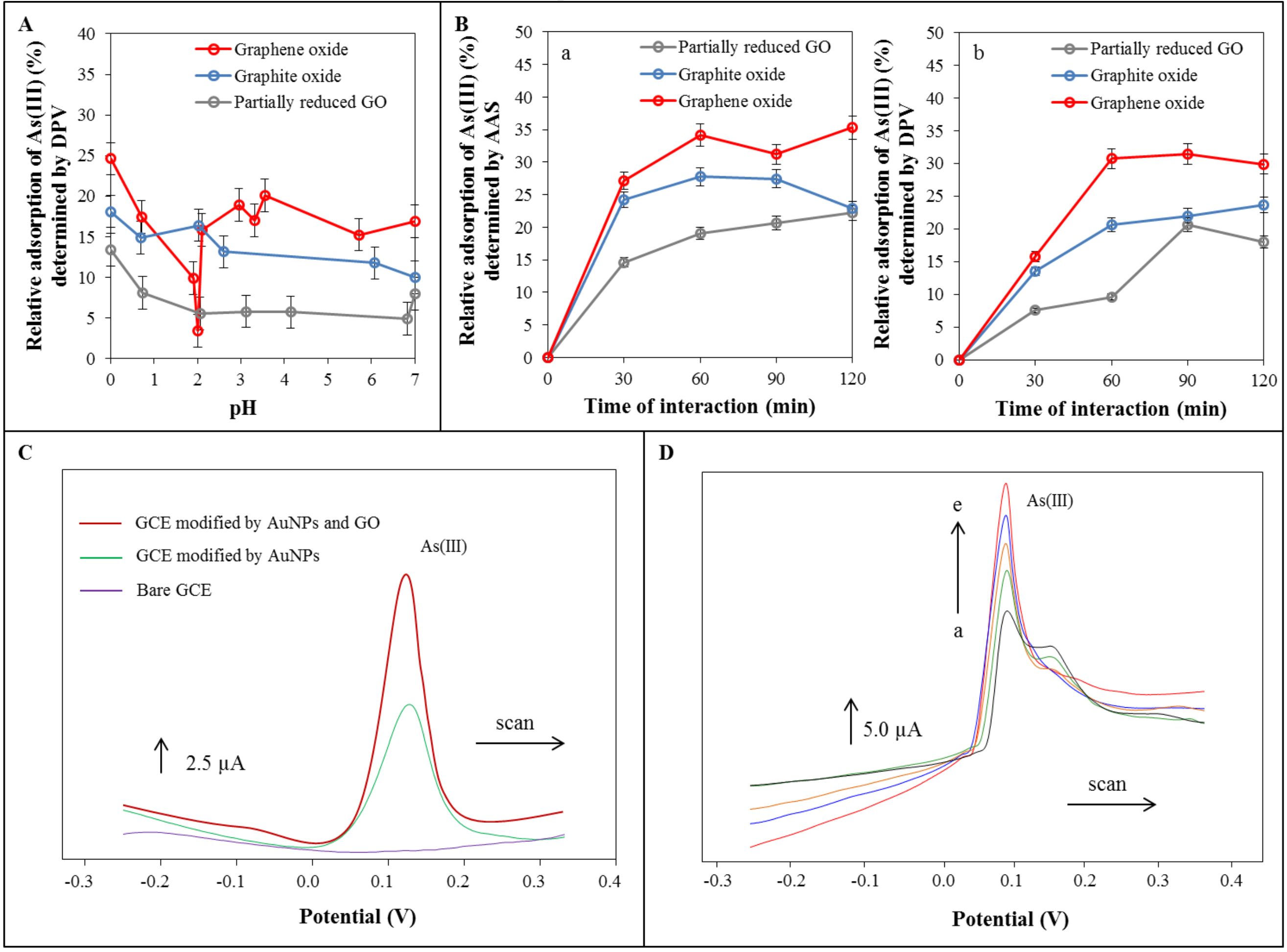

Figure 4. (A) relative adsorption of As(III) depending on pH, red line is for graphene oxide, blue line for graphite oxide, grey line for partially reduced graphene oxide, measured by differential pulse voltammetry with 0.75 M HCl as a supporting electrolyte; **(B)** relative adsorption of As(III) depending on time interaction (0; 30; 60; 90 and 120 minutes) determined by (a) atomic absorption spectrometry and (b) differential pulse voltammetry, red line is for graphene oxide, blue line for graphite oxide, grey line for partially reduced graphene oxide; **(C)** voltammograms of As(III) signal determined using bare GCE (violet line), GCE modified by AuNPs (green line) and GCE modified by AuNPs and GO (red line), measured by linear sweep voltammetry in 0.75 M HCl as a supporting electrolyte, parameters of the method were as follows: initial potential of -0.4 V, end potential 0.5 V, sample interval 0.001 V, preconditioning potential -0.4 V, deposition time 60 s, scan rate 0.1 V/s; **(D)** voltammograms of As(III) signal depending on time interaction with GO on the GCE surface, (a) 0 minutes, black line, (b) 15 minutes, green line, (c) 30 minutes, orange line, (d) 45 minutes, blue line, (e) 60 minutes, red line.

3.4. The behaviour of As(III) on glassy carbon electrode modified with gold nanoparticles and graphene oxide

For As(III) detection on glassy carbon electrode, it is necessary to modify electrode surface by some substance with higher affinity to this transition metal, e.g. AuNPs because using bare GCE led to the no electrochemical signal for As(III) [55,56]. Using the results obtained from analysis of the interaction between arsenic and carbon-based materials (determined on hanging mercury drop electrode), the glassy carbon electrode was modified using gold nanoparticles followed by graphene oxide, which was selected as the material with the highest efficiency of As(III) adsorption on its surface. At each change made to the surface of the glassy carbon electrode, this electrode was involved in the electrochemical cell as a working electrode, and the electrochemical response of As(III) in standard solution was detected. Figure 4C shows that the glassy carbon electrode without any modification makes no electrochemical signal of As(III), Sakira et al shows the same trend on solid carbon paste electrode [57]. Modification of gold nanoparticles (10-15 nm) was carried out by applying AuNPs solution and evaporation of the liquid at 30°C. After this adjustment an electrochemical signal of As(III) was recorded. In the next step, dual modification of the surface was made using AuNPs and graphene oxide. After this modification, the electrochemical signal of arsenic increased by more than 50% compared to the initial signal of As(III) on gold nanoparticles. This effect could be seen also in Liu et al. article, where authors used electrodeposition as alternative possibility of glassy carbon electrode modification [58].

To verify the process of As(III) adsorption glassy carbon electrode modified by AuNPs and GO was immersed into the electrolyte (0.75 M HCl) containing As(III) ions at concentration of 1 μg/mL. At times 0; 15; 30; 45; 60 minutes an electrochemical signal of As(III) in the mixture was measured (Figure 4D). The initial signal of As(III) measured at time 0 was increased with increasing interaction time. Electrochemical signal reached a maximum in 60 minutes, after that in the case of longer interaction times (data for 75 and 90 minutes not presented) peak height of As(III) did not increase. It is possible to say that after 60 minutes of interaction, the surface of graphene oxide was saturated by As(III) ions.

4. CONCLUSIONS

Due to its toxicity and carcinogenicity, arsenic is considered one of the major environmental threats of this millennium. With regard to the environmental importance of arsenic, it still makes sense to seek new ways of detection and it is also important to design methods that allow rapid, inexpensive, routine detection of this element. In this study, an alternative method for detection of As(III) using GC/AuNPs/GO electrode has been proposed. This method of double modification resulted in a two-fold increase of the electrochemical signal of As(III) in comparison with a simple modification of GCE using gold nanoparticles only.

ACKNOWLEDGEMENTS

Financial support from CEITEC CZ.1.05/1.1.00/02.0068 is greatly acknowledged.

CONFLICT OF INTEREST

The authors have declared no conflict of interest.

References

1. S. Wang, C. N. Mulligan, *Sci. Total Environ.*, 366 (2006) 701.
2. K. R. Raj, S. Saxena, A. Kardam, S. P. Satsangi, S. Srivastava, *Clean Technol. Environ. Policy, 1*6 (2014) 377.
3. A. Vahidnia, G. B. Van der Voet, F. A. de Wolf, *Hum. Exp. Toxicol.*, 26 (2007) 823.
4. C. A. Morrissey, J. E. Elliott, in J.E. Elliott, C.A. Bishop, C.A. Morrissey (Editors), Wildlife Ecotoxicology: Forensic Approaches, Springer, New York (2011).
5. M. F. Hughes, B. D. Beck, Y. Chen, A. S. Lewis, D. J. Thomas, *Toxicol. Sci.*, 123 (2011) 305.
6. H. Kaur, R. Kumar, J. N. Babu, S. Mittal, *Biosens. Bioelectron.*, 63 (2015) 533.
7. C. H. Tseng, *Toxicol. Appl. Pharmacol.*, 235 (2009) 338.
8. P. Andrewes, W. R. Cullen, E. Polishchuk, *Environ. Sci. Technol*., 34 (2000) 2249.
9. S. Y. Zhang, G. X. Sun, X. X. Yin, C. Rensing, Y. G. Zhu, *Chemosphere*, 93 (2013) 47.
10. S. Maeda, K. Kusadome, H. Arima, A. Ohki, K. Naka, *Appl. Organomet. Chem*., 6 (1992) 407.
11. L. Rodriguez-Lado, G. F. Sun, M. Berg, Q. Zhang, H. B. Xue, Q. M. Zheng, C. A. Johnson, *Science*, 341 (2013) 866.
12. U. K. Chowdhury, B. K. Biswas, T. R. Chowdhury, G. Samanta, B. K. Mandal, G. C. Basu, C. R. Chanda, D. Lodh, K. C. Saha, S. K. Mukherjee, S. Roy, S. Kabir, Q. Quamruzzaman, D. Chakraborti, *Environ. Health Perspect*., 108 (2000) 393.
13. P. N. Williams, M. R. Islam, E. E. Adomako, A. Raab, S. A. Hossain, Y. G. Zhu, J. Feldmann, A. A. Meharg, *Environ. Sci. Technol.*, 40 (2006) 4903.
14. P. N. Williams, S. Islam, R. Islam, M. Jahiruddin, E. Adomako, A. R. M. Soliaman, G. Rahman, Y. Lu, C. Deacon, Y. G. Zhu, A. A. Meharg, *Environ. Sci. Technol*., 43 (2009) 8430.
15. P. N. Williams, M. Lei, G. X. Sun, Q. Huang, Y. Lu, C. Deacon, A. A. Meharg, Y. G. Zhu, *Environ. Sci. Technol*., 43 (2009) 637.
16. B. L. Rivas, M. D. Aguirre, *Water Res.*, 44 (2010) 5730.
17. H. A. Michael, *Science*, 341 (2013) 852.
18. Z. Ning, D. T. Lobdell, R. K. Kwok, Z. Liu, S. Zhang, C. Ma, M. Riediker, J. L. Mumford, T*oxicol. Appl. Pharmacol*., 222 (2007) 351.
19. A. Smith, P. Lopipero, J. Chung, R. Haque, A. Hernandez, L. Moore, C. Steinmaus, *Epidemiology*, 11 (2000) S93.
20. R. Stone, *Science*, 321 (2008) 184.
21. Y. G. Zhu, P. N. Williams, A. A. Meharg, *Environ. Pollut.*, 154 (2008) 169.
22. P. B. Tchounwou, A. K. Patlolla, J. A. Centeno, *Toxicol. Pathol.*, 31 (2003) 575.
23. M. Sun, G. J. Liu, Q. H. Wu, W. Q. Liu, *Talanta*, 106 (2013) 8.
24. M. I. An, M. L. Chen, J. H. Wang, *Chin. J. Anal. Chem*., 41 (2013) 105.
25. C. G. Yuan, B. He, E. L. Gao, J. X. Lu, G. B. Jiang, *Microchim. Acta*, 159 (2007) 175.
26. H. W. Sun, X. L. Liu, Y. Y. Miao, *Food Anal. Meth.*, 4 (2011) 251.
27. I. Hagarova, M. Bujdos, L. Canecka, P. Matus, *Fresenius Environ. Bu*ll., 20 (2011) 2927.
28. M. M. Wolle, G. M. M. Rahman, H. M. Kingston, M. Pamuku, *Anal. Chim. Acta,* 818 (2014) 23.
29. M. Han, G. X. Zhao, S. Z. Li, Z. H. Sun, Y. Li, N. Jia, *Chin. J. Anal. Chem*., 41 (2013) 1780.
30. J. Tyson, *Spectroscopy*, 28 (2013) 40.

31. B. Norshidah, S. Norashikin, O. Rozita, Z. S. Md, J. Hafizan, S. R. Saari, *Res. J. Chem. Environ.*, 15 (2011) 45.
32. C. Niegel, S. A. Pfeiffer, M. Grundmann, U. Arroyo-Abad, J. Mattusch, F. M. Matysik, *Analyst*, 137 (2012) 1956.
33. G. Henze, W. Wagner, S. Sander, Fresenius *J. Anal. Chem*., 358 (1997) 741.
34. M. Zaib, A. Saeed, I. Hussain, M. M. Athar, M. Iqbal, *Biosens. Bioelectron.*, 62 (2014) 242.
35. J. C. M. Gamboa, L. Cornejo, J. A. Squella, *J. Appl. Electrochem.*, 44 (2014) 1255.
36. Z. G. Liu, X. J. Huang, *Trac-Trends Anal. Chem*., 60 (2014) 25.
37. M. C. Teixeira, E. D. L. Tavares, A. A. Saczk, L. L. Okumura, M. D. Cardoso, Z. M. Magriotis, M. F. de Oliveira, *Food Chem.*, 154 (2014) 38.
38. Y. C. Lan, H. J. Luo, X. H. Ren, Y. P. Wang, Y. Z. Liu, *Microchim. Acta*, 178 (2012) 153.
39. T. Tanaka, T. Sato, T. Ishiyama, *Tetsu To Hagane-J. Iron Steel Inst. Jpn.*, 85 (1999) 129.
40. S. Prakash, T. Chakrabarty, A. K. Singh, V. K. Shahi, *Electrochim. Acta*, 72 (2012) 157.
41. W. S. Hummers, R. E. Offeman, *J. Am. Chem. Soc.*, 80 (1958) 1339.
42. H. N. Lim, N. M. Huang, C. H. Loo, *J. Non-Cryst. Solids*, 358 (2012) 525.
43. W. Gao, L. B. Alemany, L. J. Ci, P. M. Ajayan, *Nat. Chem*., 1 (2009) 403.
44. D. T. Nguyen, D. J. Kim, M. G. So, K. S. Kim, *Adv. Powder Technol*., 21 (2010) 111.
45. X. Wang, B. Liu, Q. P. Lu, Q. S. Qu, *J. Chromatogr.*, A 1362 (2014) 1.
46. L. Liu, C. Li, C. L. Bao, Q. Jia, P. F. Xiao, X. T. Liu, Q. P. Zhang, *Talanta*, 93 (2012) 350.
47. L. Y. Hao, H. J. Song, L. C. Zhang, X. Y. Wan, Y. R. Tang, Y. Lv, *J. Colloid Interface Sci.*, 369 (2012) 381.
48. E. Palecek, M. Bartosik, *Chem. Rev.*, 112 (2012) 3427.
49. I. M. Ritchie, S. Bailey, R. Woods, *Adv. Colloid Interface Sci.*, 80 (1999) 183.
50. D. Fialova, M. Kremplova, L. Melichar, P. Kopel, D. Hynek, V. Adam, R. Kizek, *Materials*, 7 (2014) 2242.
51. D. Fialova, M. Kremplova, D. Hynek, M. Konecna, J. Kaiser, R. Malina, J. Kynicky, O. Krystofova, R. Kizek, V. Adam, *Int. J. Electrochem. Sci*., 8 (2013) 7853.
52. C. Piloto, M. Notarianni, M. Shafiei, E. Taran, D. Galpaya, C. Yan, N. Motta, Beilstein *J. Nanotechnol*., 5 (2014) 1073.
53. E. D. Burton, R. T. Bush, S. G. Johnston, K. M. Watling, R. K. Hocking, L. A. Sullivan, G. K. Parker, *Environ. Sci. Technol.*, 43 (2009) 9202.
54. J.-M. Beralus, R. Ruiz Rosas, D. Cazorla-Amoros, E. Morallon, *Front. Mater*., 1 (2014)
55. A. N. Chowdhury, S. Ferdousi, M. M. Islam, T. Okajima, T. Ohsaka, *J. Appl. Polym. Sci.*, 104 (2007) 1306.
56. M. M. Hossain, M. M. Islam, S. Ferdousi, T. Okajima, T. Ohsaka, *Electroanalysis*, 20 (2008) 2435.
57. A. K. Sakira, I. T. Some, E. Ziemons, B. Dejaegher, D. Mertens, P. Hubert, J. M. Kauffmann, *Electroanalysis*, 27 (2015) 309.
58. Y. Liu, Z. Huang, Q. J. Xie, L. E. Sun, T. A. Gu, Z. Li, L. J. Bu, S. Z. Yao, X. M. Tu, X. B. Luo, S. L. Luo, *Sens. Actuator B-Chem*., 188 (2013) 894.